IEEE Access
Multidisciplinary | Rapid Review | Open Access Journal

Received August 15, 2020, accepted August 22, 2020, date of publication August 25, 2020, date of current version September 10, 2020.

Digital Object Identifier 10.1109/ACCESS.2020.3019416

Evaluation of Characterization Indexes and Minor Looseness Identification of Flange Bolt Under Noise Influence

XIE JIANG[1], XIN ZHANG[1,2], AND YUXIANG ZHANG[1]

[1]Xi'an Research Institute of Hi-Tech, Xi'an 710025, China
[2]Northwest Institute of Nuclear Technology, Xi'an 710024, China

Corresponding authors: Xin Zhang (xinzhang@hit.edu.cn) and Yuxiang Zhang (sxbbm201601@126.com)

This work was supported by the National Natural Science Foundation of China under Grant 51975581.

ABSTRACT Based on electromechanical impedance (EMI) technology, we studied the indication effect of each characterization index on flange bolt looseness under different noise levels. A new evaluation index T is constructed to solve the problem that the minor looseness and noise under the actual monitoring environment cannot be distinguished with existing indexes. The results show that among the five characterization indexes, the root mean square deviation (RMSD) and the correlation coefficient deviation (CCD) can reflect the minor looseness sensitively and are positively correlated with the degree of looseness. They also have good performance of looseness identification under the noise of 30 dBW. However, the indexes' indication range of the case under 1 dBW-6 dBW noise overlaps with the case under 36 N·m-39.5 N·m torque. So it is impossible to judge the structure state with mere characterization indexes. Evaluation index T can extract the correlation difference of the conductance spectrum under the noise conditions and looseness conditions with the benchmark respectively. And there are different indication ranges of T on the noise and minor looseness. By determining a threshold and comparing T with it, whether bolt looseness occurs in an unknown condition can be effectively judged. Finally, T is applied to other flange structure with 8 bolts to verify the effectiveness and general applicability of the method. The evaluation index plays an important role in avoiding misjudgment of flange bolt caused by noise influence on minor looseness and improving the ability of identification when the bolt is at the critical state.

INDEX TERMS Electromechanical impedance technology, flange bolt monitoring, minor looseness, noise influence, evaluation index T.

I. INTRODUCTION

Bolt connection has been widely used in various engineering practices for its convenience of assembling and disassembling. And flange bolt is the main way of pipeline connection. Currently, the main reason for pipeline leakage accidents is the sealing failure caused by the loose bolt. Therefore, it is of great engineering significance to realize online monitoring and evaluation of flange bolt looseness. Piezoelectric ceramics, as a new intelligent monitoring material [1], has attracted the attention of researchers for its high cost performance, low power, no damage to the structure, good long-term stability, ability of online monitoring, and other advantages. Some researches had verified its application to the actual space structure [2], including truss structure [3], pin connection [4], concrete structure [5], bolt structure [6], and so on.

Bolt loosening monitoring has been researched in many papers. Wang *et al.* [7] proposed an active sensing method based on piezoelectric ceramics and verified its feasibility on bolt connection state detection by analyzing the received energy. Zhang *et al.* [8] used LibSVM to process impedance data, which effectively improves the detection sensitivity of electromechanical impedance (EMI) to bolt looseness. Shao *et al.* [9] determined 35 kN as the maximum load of the bolt then set eight load steps from 0 kN to 35 kN. And the results show a linear and negative relationship between the preload and the peak frequency. Wang *et al.* [10], [11] used fractal contact theory to calculate the mechanical impedance of bolt connection under different preload and realized quantitative monitoring of looseness.

The associate editor coordinating the review of this manuscript and approving it for publication was Yu Liu.

This work is licensed under a Creative Commons Attribution 4.0 License. For more information, see https://creativecommons.org/licenses/by/4.0/

Ritdumrongkul and Fujino *et al.* [12] established a structural model by adopting the spectral element method, which is used to identify the location and degree of damage quantitatively. Pavelko *et al.* [13] pasted piezoelectric lead zirconate titanate (PZT) patch on the tail beam of the aircraft and studied the bolts with electromagnetic interference method. They found that the looseness would lead to significant changes in electromagnetic interference measurement values. To infer bolt loosening state, Yin *et al.* [14] observed the peak amplitude change of focus signal when the transmitted wave energy of the bolt connection interface changed. Rabiei *et al.* [15] quantified and positioned the bolt looseness on launching bridge of armored vehicle through the PZT network distributed on the structure. Through experiments, Samantaray *et al.* [16] verified the feasibility of PZT application in the condition monitoring of the railway bolted structure based on the electromagnetic interference method.

For the detection of flange bolt looseness, Tang *et al.* [17] took 40 N·m as a benchmark and set eight testing groups from 0 N·m to 35 N·m. He then defined a new damage index RMSCR and proved that it is little affected by the structural difference. Martowicz *et al.* [18] analyzed the different damage conditions related to the loose bolts and the measurement configuration. By applying the point frequency response function and transferring frequency response function, he made the qualitative and quantitative analysis of random damage.

In the study of structural damage signal extraction under noise environment, Bastani *et al.* [19] proposed a method using sensor array and statistical metric analysis to identify signal changes derived from damage and/or environmental change and showed its reliability to identify damage. Campeiro *et al.* [20] evaluated the influence of noise and vibration on impedance characteristics by calculating the coherence function and basic damage index. De Castro *et al.* [21] first applied the Hinkley criterion as a new feature extraction method to structural health monitoring (SHM) based on impedance under low signal-noise ratio (SNR). It was proved that the method is more sensitive to structural damage than basic damage index and wavelet transform in the noise environment. Then they proposed another new method to extract structural features by combining the chromatic technique with the Hinkley criterion to promote the accuracy of damage diagnosis based on impedance measurement under different noise levels [22]. However, the Hinkley criterion is generally used to detect the change of the time-domain signal. By comparing the characteristics of baseline signal and noise signal, De Castro *et al.* [23] established a new damage index cross-correlation square deviation (CCSD) which can extract structural damage information from mere impedance frequency-domain signal.

The above methods lead to the conclusion that it is simple and feasible to monitor the flange bolt looseness by using characterization indexes. Xu [24] and Wang [25] show different identification ability of characterization indexes on girder and concrete. As for the flange bolt, there are still many problems need further study, for example, the capacity of indexes to represent looseness degree under different noise levels, whether each characterization index is able to distinguish minor looseness and noise, as well as the necessity to create a new index to judge the structure condition.

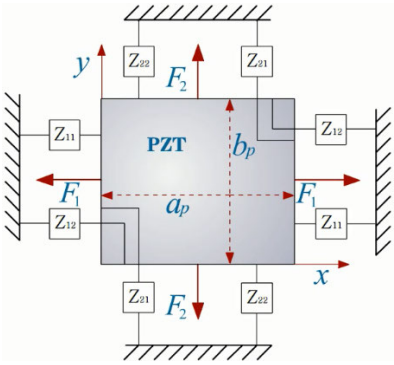

FIGURE 1. The two-dimensional EMI model.

II. MONITORING PRINCIPLE AND CHARACTERIZATION INDEXES OF ELECTROMECHANICAL IMPEDANCE METHOD

A. DETECTION TECHNOLOGY BASED ON ELECTROMECHANICAL IMPEDANCE METHOD

Liang *et al.* [26] concluded that the coupling system of PZT and structure under test is possible to be simplified into a one-dimensional model of the mass-stiffness-damping system when only axial deformation is considered. Zhou [27], Zagrai [28], and Yang [29] then respectively extended Liang's model to a two-dimensional model, which is the same solution process like the one in the one-dimensional model. In the analysis of the two-dimensional structure, the inertial forces in two directions of the PZT are considered, which makes the solution of the conductance spectrum closer to the real situation. Two-dimensional EMI model and admittance expressions are shown in Fig. 1 and (1)-(3), as shown at the bottom of the next page. In the above equations, $Y(\omega)$ = admittance; j = imaginary part of a complex number; ω = excitation angular frequency at work; μ_p = Poisson's ratio of the PZT material; b_p, a_p, and h_p = length, width, and thickness of PZT; $\bar{\varepsilon}_{33}^T = \varepsilon_{33}^T(1 - j\delta)$ = complex dielectric constant at constant stress, ε_{33}^T = dielectric constant, δ = dielectric loss factor; $\bar{Y}_p^E = Y_p^E(1 + j\eta)$ = complex Young's modulus of PZT at zero-elastic field, Y_p^E = real Young's modulus, η = mechanical loss factor; d_{31} and d_{32} = piezoelectric constants and $d_{31} = d_{32}$ is usually assumed; $K_p = \omega\sqrt{\rho_p/\bar{Y}_p^E}$ = wave number, ρ_p = mass density of the PZT; A and C = unknown coefficients determined from the boundary conditions. For a certain system, the above parameters are fixed values. I = identity matrix of 2×2; Z_{11} and Z_{22} = direct mechanical impedance of the structure; Z_{12} and Z_{21} = cross mechanical impedance of the structure. Since the states of piezoelectric components and

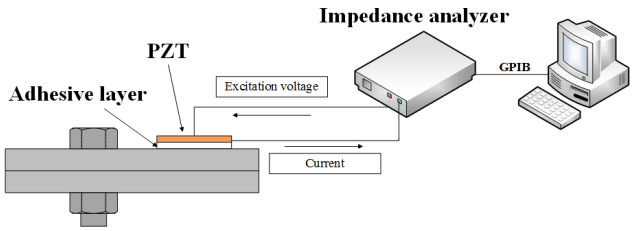

FIGURE 2. Schematic diagram of flange bolt looseness detection experimental devices.

bonding layers are usually stable, it can be concluded that the electrical admittance of a three-layer piezoelectric intelligent structure composed of piezoelectric wafers, adhesive layers, and tested structures is mainly affected by the structural mechanical impedance, i.e. the change of structural states, such as local structural damage. Therefore, piezoelectric admittance reflects the health status of the structure.

The basic principle of the EMI method in bolt looseness monitoring is [30], [31]: using the positive piezoelectric effect of PZT as the sensor and the inverse piezoelectric effect as the exciter. The PZT sensor is coupled with structure through the adhesive layer and high-frequency AC voltage generated by the impedance analyzer is applied to it. The measured structure vibrates due to the deformation of PZT which will in turn result in the coupled PZT deformation and then current generation. The electrical impedance of the coupled structure is obtained by the analyzer and then transmitted to PC by a general-purpose interface bus (GPIB) for further analysis. By comparing the electrical impedance curves, we can infer the damage information of the structure. The schematic diagram is shown in Fig. 2.

B. CHARACTERIZATION INDEXES

When the structure is damaged, the measured admittance spectrum curve will deviate from that when the structure is not damaged, and the degree of deviation reflects the degree of structural damage [32]–[34]. To characterize the damage quantitatively, the statistical indicators, regarded as characterization indexes are used to evaluate it. The main statistical indicators of damage evaluation are as follows: the root mean square deviation (RMSD) [35], [36], the root mean square of change ratio (RMSCR) [17], the mean absolute percentage deviation (MAPD) [37], [38], the correlation coefficient deviation (CCD) [35], [39], and the covariance (Cov) [28], [40] which are shown in (4)-(8) respectively. To facilitate the comparison, Cov is normalized so that its magnitude is consistent with other characterization indexes' and the ratio of Cov under various working conditions and health conditions is defined as Cov', as shown in (9).

$$RMSD = \sqrt{\sum_{N}\left[Re(Y_i) - Re(Y_i^0)\right]^2 \Big/ \sum_{N}\left[Re(Y_i^0)\right]^2} \tag{4}$$

$$RMSCR = \sqrt{\frac{1}{N}\sum_{N}\left(\frac{Re(Y_i) - Re(Y_i^0)}{Re(Y_i^0)}\right)^2} \tag{5}$$

$$MAPD = \sum_{N}\left|\left[Re(Y_i) - Re(Y_i^0)\right] \Big/ Re(Y_i^0)\right| \tag{6}$$

$$CCD = 1 - \frac{1}{N\sigma_Y\sigma_{Y^0}}\sum_{N}\left[Re(Y_i) - Re(\overline{Y})\right] \cdot \left[Re(Y_i^0) - Re(\overline{Y^0})\right] \tag{7}$$

$$Cov = \frac{1}{N}\sum_{N}\left[Re(Y_i) - Re(\overline{Y})\right] \cdot \left[Re(Y_i^0) - Re(\overline{Y^0})\right] \tag{8}$$

$$Cov_n' = \frac{Cov_n}{Cov_0} \tag{9}$$

In the formula, $Re(Y_i^0)$ and $Re(Y_i)$ = real part of the admittance before and after damage at the ith frequency point. Because the real part of the admittance has better sensitivity to structural changes than the imaginary, the change of the real part is usually used to represent structural state [41], [42]; $\overline{Y^0}$ and $\overline{Y}$ = average value of all frequency points results before and after the damage; N = number of measurement frequency points; σ_{Y^0} and σ_Y = standard deviation of all measurement points before and after damage. Cov_n and Cov_0 = values of Cov under the nth condition and reference condition respectively.

$$Y(\omega) = \frac{j\omega}{h_p}\left\{\frac{\bar{Y}_p^E}{1-\mu_p^2}\begin{bmatrix}(d_{31}+\mu_p d_{32})\left(2Ab_p\tan\dfrac{K_p a_p}{2} - d_{31}a_p b_p\right)\\ +(\mu_p d_{31}+d_{32})\left(2Ca_p\tan\dfrac{K_p b_p}{2} - d_{32}a_p b_p\right)\end{bmatrix} + \bar{\varepsilon}_{33}^T a_p b_p\right\} \tag{1}$$

$$\begin{Bmatrix}A\\C\end{Bmatrix} = M^{-1}\begin{Bmatrix}d_{31}\\d_{32}\end{Bmatrix} \tag{2}$$

where

$$M = I - \frac{j\omega}{\bar{Y}_p^E K_p h_p}\begin{bmatrix}\dfrac{Z_{11}}{b_p} - \dfrac{Z_{21}\mu_p}{a_p} & \dfrac{Z_{12}}{b_p} - \dfrac{Z_{22}\mu_p}{a_p}\\ \dfrac{-Z_{11}\mu_p}{b_p} + \dfrac{Z_{21}}{a_p} & \dfrac{-Z_{12}\mu_p}{b_p} + \dfrac{Z_{22}}{a_p}\end{bmatrix} \times \begin{bmatrix}-\tan\dfrac{k_p a_p}{2} & 0\\ 0 & -\tan\dfrac{k_p b_p}{2}\end{bmatrix} \tag{3}$$

TABLE 1. Material properties.

Material property	Symbol	PZT	carbon steel (Flange)	Unit
Mass density	ρ	7750	7850	kg/m^3
Young's modulus	E	65	206	Gpa
Poisson's ratio	μ	0.35	0.24	—
Piezoelectric constants	d_{31} ,d_{32}	0.186	—	nC/N
Dielectric constant	ε_{33}^{T}	0.15	—	nF/N
Dielectric loss factor	δ	0.02	—	—
Mechanical loss factor	η	0.001	—	—

III. EXPERIMENTAL SETUP

A. EXPERIMENTAL PRINCIPLE AND DEVICES

A designed experiment was conducted to establish the relationship between characterization indexes and bolt looseness. In the preparation step of the experiment, a PZT (Φ16 mm×2 mm) of PZT-5A (response frequency of 130 kHz) was pasted on the surface of a four bolted flange structure (Φ100 mm) with modified acrylate adhesive. The adhesive has a mass ratio of epoxy resin and a hardener of 1:1. The PZT and the flange plate were gently pressed by fingers, then were allowed to stand for 24 hours until the epoxy adhesive solidifies to make them closely fit. The size of each bolt is M24 mm×1.25 mm×60 mm. The material properties of PZT and flange are shown in Table 1.

During the measurement, the positive and negative electrodes are led out on the surface of PZT which are also connected with the WK6500B impedance analyzer clamp. The excitation voltage range of the analyzer is 10 mV-1 V. In a certain range, choosing a higher excitation voltage can significantly increase the detection sensitivity of the EMI method [43], [44]. The upper limit excitation voltage of impedance analyzer 1 V was selected to make the detection more sensitive in the experiment, which excites PZT, thus causing PZT deformation and the vibration of the coupling structure. The collected result reflects the relationship between the looseness and the signal of PZT. For the choice of the frequency band ranges, a test on a wide frequency band of 20 Hz-1 MHz was carried out at first. By observing and comparing the conductance curves of PZT under different working conditions in different frequency bands, frequency ranges of 350 kHz-650 kHz were found for the densest distribution of resonance peaks and the most sensitive to the looseness change of flange bolt. Besides, under the high-frequency range, the wavelength of excitations is small and sensitive enough to detect minor changes in structural integrity [45]. 400 points are evenly sampled in the frequency range. In consideration of the fact that the possibility of a sudden torque change is relatively small when the bolt is loose, nine torque levels from 40 N·m

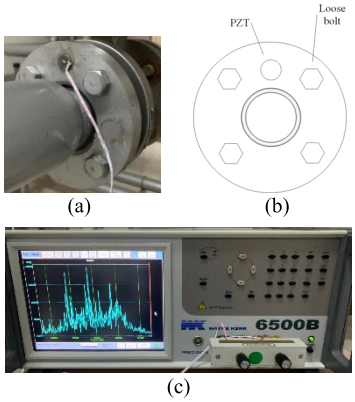

FIGURE 3. The experimental devices include (a) a four bolted flange with PZT whose layout diagram is shown in (b) and (c) WK6500B precision impedance analyzer.

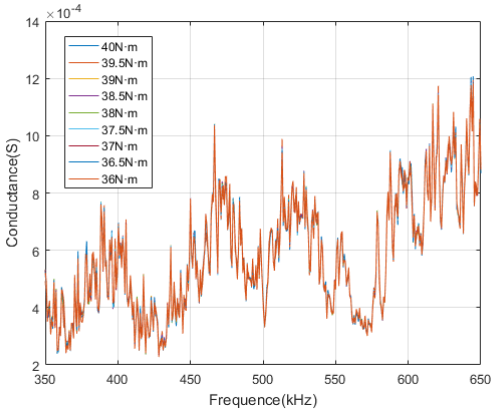

FIGURE 4. The conductance spectrum curves under 36 N·m-40 N·m torque with a frequency of 350 kHz-650 kHz.

to 36 N·m with decrements of 0.5 N·m were applied by a torque wrench. Among them, 40 N·m torque was set as a benchmark. Additionally, to reduce random error and to avoid the influence of temperature change on the signal, each torque condition was measured five times under a constant temperature of 26 °C, and the average value of the characterization indexes was obtained.

To further study the influence of noise on the indication effect of each characterization index, noise is added to the output signal and the signal expression is:

$$G_{ni} = G_{0i} + X_{ni} \tag{10}$$

where, G_{0i} and G_{ni} = value of the ith frequency point of the conductance before and after adding the nth noise respectively; X_{ni} = level of the nth noise at the corresponding frequency point; dBW = unit of X_{ni} = 10 log (P/1w), where P = power, w = unit Watt. To explore the identification capacity of characterization indexes under different noise levels, combined with the actual noise levels of fuel pipeline filling process, Gaussian white noise (5, 10, 15, 20, 25, 30 dBW) is superimposed on the conductance spectrum in turn. Furthermore, noise (1, 2, 3, 4, 5, 6 dBW) is added to the signal in sequence to find out whether the existing indexes can

TABLE 2. Characterization indexes under different torque.

Torque (N·m)	RMSD	RMSCR	MAPD	CCD	Cov	Cov′
36	3.955	4.578	3.469	0.721	4.08E-06	1.0007
36.5	2.694	3.039	2.312	0.335	4.10E-06	0.9976
37	1.302	1.634	1.108	0.078	4.09E-06	0.9989
37.5	1.193	1.494	1.028	0.066	4.09E-06	0.9997
38	1.165	1.479	1.012	0.063	4.10E-06	1.0001
38.5	1.163	1.439	1.01	0.062	4.09E-06	1.0003
39	0.984	1.227	0.81	0.045	4.09E-06	1.0001
39.5	0.89	1.164	0.712	0.037	4.09E-06	0.9993
40	0.595	0.803	0.476	0.016	4.09E-06	1

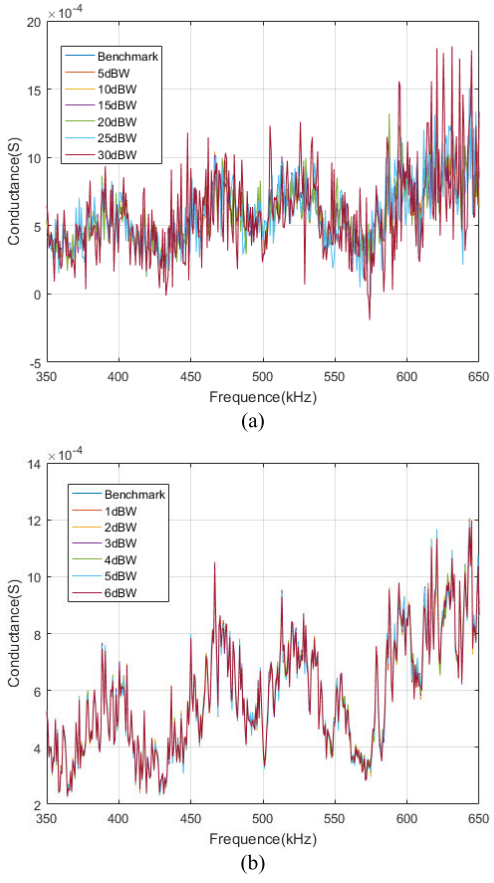

FIGURE 5. The influence of different noise levels (a) 5 dBW-30 dBW and (b) 1 dBW-6 dBW on the conductance spectrum.

distinguish minor looseness from noise when both of them may have a similar impact on the conductance spectrum.

B. EXPERIMENTAL RESULT

The conductance spectrum curves under nine working conditions are shown in Fig. 4. With 40 N·m as the benchmark, characterization indexes under different working conditions were calculated in Table 2. Taking 38.5 N·m as an example, the influence of different noise levels on the conductance spectrum is shown in Fig. 5.

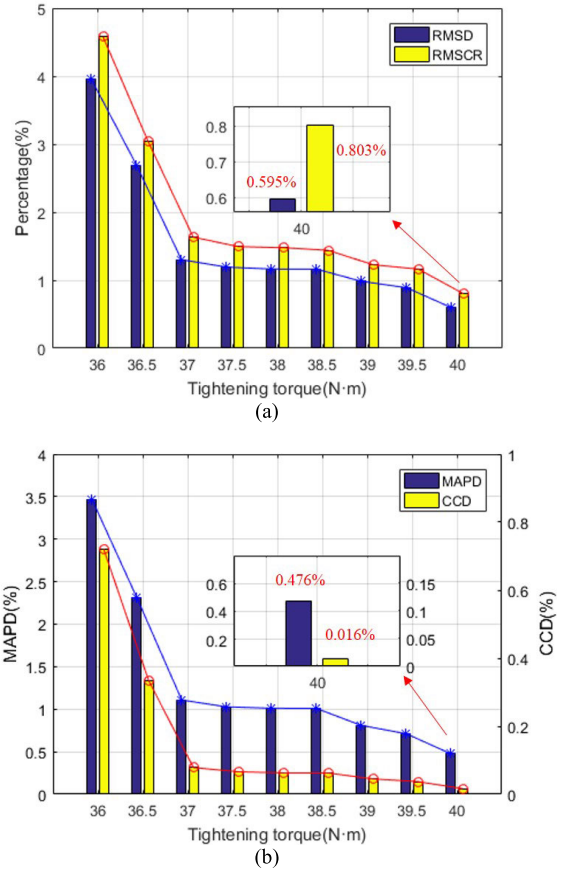

FIGURE 6. (a) RMSD, RMSCR and (b) MAPD, CCD under 36 N·m-40 N·m torque with a partially enlarged view at 40 N·m.

IV. CHARACTERIZATION EFFECT ANALYSIS AND EVALUATION INDEX PROPOSED

A. MINOR LOOSENESS ANALYSIS

According to Fig. 4, the connection state cannot be characterized by the peak frequency of the conductance spectrum as it does not show a positive correlation with the increase of bolt preload [9].

The characterization indexes under different working conditions are compared without adding noise. The data in Table 2 is represented by a histogram in Fig. 6. In two figures, the horizontal axis is the bolt tightening torque and the vertical axis is the corresponding index identification percentage. The identification capacity of each index is preliminarily judged by comparing the height of the histogram under each working condition.

Fig. 6 points out that with the increase of looseness, the values of the first four characterization indexes are also larger when the difference between adjacent preloading moments is 0.5 N·m. It shows the above characterization indexes effectively identify looseness and have certain sensitivity. However, the value of Cov'changes irregularly under various working conditions thus it cannot reflect looseness. In the qualitative and quantitative test of flange bolt looseness, this statistical indicator cannot be taken as a characterization index.

B. NOISE IMPACT STUDY

Ten groups of data were collected under 40 N·m torque among which the average of 5 groups was taken as a benchmark, and the others were taken as the tested groups. In the study, the benchmark is approximated to the data obtained in the noise-free environment. As two groups of data were obtained under the same torque condition, two curves of the conductance spectrums may also overlap. However, it can be seen from Fig. 6 that when the torque is 40 N·m, the characterization indexes are not zero. Combined with the experimental principle and environment, the following reasons are analyzed. Firstly, improving the sweep range and repeating the experiments cannot eliminate all environmental noise which leads to the irreducible random error of the measurement. Secondly, the indexes are easy to extract the subtle influence of noise as a structure looseness feature on the conductance spectrum. For a better comparison of the environmental noise influence degree on indexes, the data under 40 N·m are normalized and the relative value of indexes reflects the influence degree. The larger the normalized value is, the greater the influence of noise on the index is, and vice versa. After calculation, the normalized indexes of RMSD, RMSCR, MAPD, and CCD are 0.150, 0.175, 0.137, and 0.022 under 40 N·m torque. Through the comparison of the data, it is concluded that the noise has the greatest impact on RMSCR and the least impact on CCD. The results of each index under different noise levels are shown in the table below. The comparison of the indication effect is shown in the following histogram.

TABLE 3. RMSD affected by noise.

Torque (N·m)	5dBW	10dBW	15dBW	20dBW	25dBW	30dBW
36	3.957	3.950	3.979	3.906	3.879	3.628
36.5	2.696	2.693	2.707	2.667	2.619	2.448
37	1.304	1.305	1.313	1.291	1.258	1.170
37.5	1.194	1.195	1.202	1.180	1.156	1.072
38	1.166	1.169	1.173	1.152	1.133	1.063
38.5	1.163	1.166	1.170	1.152	1.125	1.057
39	0.981	0.987	0.991	0.969	0.933	0.851
39.5	0.888	0.892	0.896	0.887	0.857	0.782
40	0.596	0.598	0.603	0.596	0.585	0.532

TABLE 4. RMSCR affected by noise.

Torque (N·m)	5dBW	10dBW	15dBW	20dBW	25dBW	30dBW
36	4.566	4.581	4.615	4.544	4.883	17.476
36.5	3.027	3.040	3.056	3.002	3.314	9.570
37	1.630	1.630	1.646	1.662	2.112	8.370
37.5	1.495	1.493	1.503	1.468	1.603	15.338
38	1.478	1.477	1.482	1.468	2.080	13.525
38.5	1.436	1.434	1.450	1.454	1.524	6.608
39	1.229	1.221	1.229	1.221	1.608	11.854
39.5	1.162	1.161	1.170	1.176	1.639	17.346
40	0.800	0.800	0.800	0.798	0.893	10.611

TABLE 5. MAPD affected by noise.

Torque (N·m)	5dBW	10dBW	15dBW	20dBW	25dBW	30dBW
36	3.465	3.466	3.487	3.444	3.640	4.865
36.5	2.306	2.310	2.330	2.292	2.462	3.158
37	1.106	1.107	1.115	1.116	1.213	1.767
37.5	1.028	1.027	1.035	1.019	1.073	2.045
38	1.010	1.011	1.020	1.011	1.056	1.500
38.5	1.009	1.009	1.016	1.008	1.106	1.950
39	0.810	0.809	0.814	0.809	0.886	1.682
39.5	0.711	0.711	0.717	0.715	0.787	1.885
40	0.476	0.475	0.477	0.474	0.504	1.138

TABLE 6. CCD affected by noise.

Torque (N·m)	5dBW	10dBW	15dBW	20dBW	25dBW	30dBW
36	0.728	0.721	0.715	0.648	0.514	0.319
36.5	0.338	0.336	0.332	0.304	0.236	0.145
37	0.079	0.079	0.078	0.071	0.054	0.033
37.5	0.067	0.067	0.066	0.060	0.046	0.028
38	0.064	0.064	0.063	0.057	0.044	0.028
38.5	0.063	0.063	0.062	0.057	0.043	0.027
39	0.045	0.046	0.045	0.040	0.030	0.018
39.5	0.037	0.037	0.037	0.034	0.026	0.015
40	0.017	0.017	0.017	0.015	0.012	0.007

The effects of different noise levels on indexes are not the same. RMSD and CCD increase as the degree of looseness increase in the noise range of 30 dBW, which shows a positive correlation with looseness and certain anti-interference ability. In the x-axis direction, the two indexes show a downward trend when the noise level grows higher, which indicates the sensitivity reduction of the indexes to looseness under the influence of noise; For RMSCR and MAPD, when the noise below 25 dBW and 25 dBW respectively, it is effective for the two indexes to looseness quantification. Whereas when the noise exceeds the corresponding upper limit, the indexes under some working conditions fail to quantify looseness. When the noise exceeds 30 dBW, the irregular fluctuation amplitude of the index increases in the direction of the horizontal and vertical axes, which leads to the wrong diagnosis. It shows that the two indexes are not able to effectively extract the structural features under influence of strong noise.

To research the effect of noise levels on different characterization indexes under the same torque condition, noise (1, 2, 3, 4, 5, 6 dBW) was added in turn with 40 N·m unchanged. The results are shown in Table 7 and Fig. 8. With the enhancement of noise, the first four indexes increase correspondingly. Cov' is excluded for its disability to reflect the noise levels. However, the characterization range under 1 dBW-6 dBW noise is included in the range of 36.5 N·m-39.5 N·m torque. By merely comparing the value of indexes, it is impossible to distinguish looseness from noise.

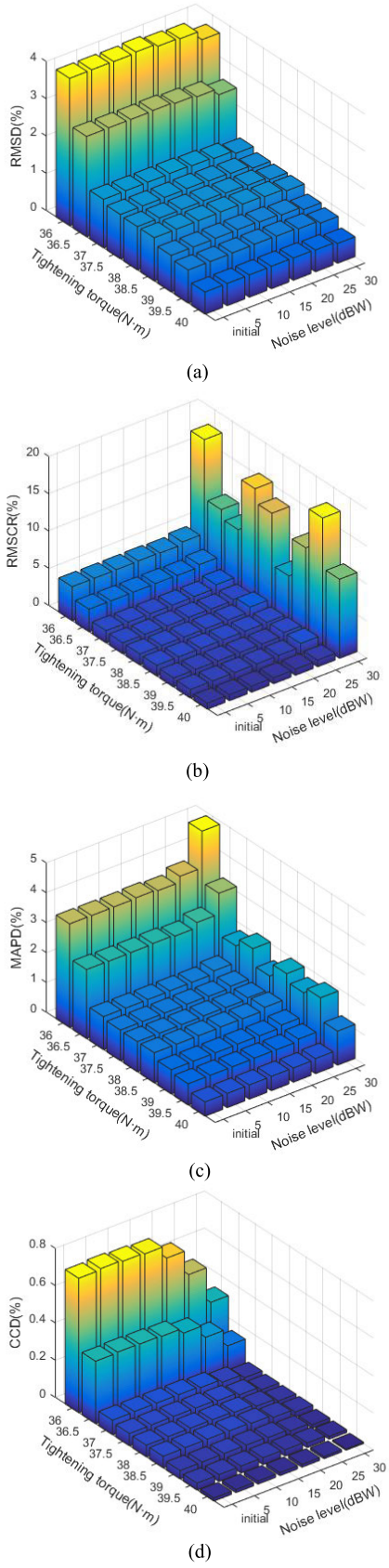

FIGURE 7. Recognition effect of (a) RMSD, (b) RMSCR, (c) MAPD, and (d) CCD on bolt looseness (36 N·m-40 N·m) under 5 dBW-30 dBW noise.

TABLE 7. Characterization indexes under different noise levels.

Noise (dBW)	RMSD	RMSCR	MAPD	CCD	Cov′
1	1.512	1.640	1.237	0.106	1.002
2	1.707	1.882	1.424	0.134	0.999
3	1.834	1.957	1.53	0.156	1.007
4	2.189	2.317	1.733	0.220	0.999
5	2.205	2.420	1.811	0.226	1.001
6	2.582	2.813	2.200	0.305	0.998

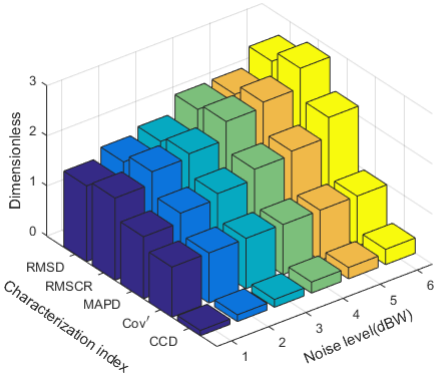

FIGURE 8. Characterization indexes change under the noise of 1 dBW-6 dBW.

C. PUT FORWARD THE EVALUATION INDEX

Because the environmental noise still has a great influence on the characterization indexes to judge whether the minor looseness occurs or not, the traditional indexes are limited in the extraction of structural features. Therefore, it is necessary to construct a new index which can distinguish noise and minor looseness and truly reflect the structural state. The conductance spectrum is amplified partly to observe the difference between the benchmark curve and the ones under other working conditions, as shown in Fig. 9.

It can be seen from Fig. 9(a) that the conductance spectrum obtained under looseness has similar behavior with the benchmark in frequency, phase, and amplitude. In other words, they have a strong correlation. However, in Fig. 9(b), the noise destroys the characteristics of the original benchmark [21]–[23], [46], [47], [48], which makes the correlation between the noise conductance spectrum and the benchmark worse than that under the loose condition. Based on this idea, the evaluation index T is constructed and its expression is as follows:

$$\mathrm{T} = \frac{\sum_{2N-1} |C\left(G_M, G_1\right) - C\left(G_1, G_1\right)|}{\left(\sigma_M - \sigma_1\right)^2} \tag{11}$$

In the formula, $C\left(G_M, G_1\right)$ = cross-correlation between the conductance of the measurement result and the conductance of benchmark; $C\left(G_1, G_1\right)$ = autocorrelation of the benchmark conductance; σ_M and σ_1 = standard deviation of all measuring points under various working conditions and benchmarks; N = number of sampling points. The T calculation for noise and the loose condition is shown in Fig. 10.

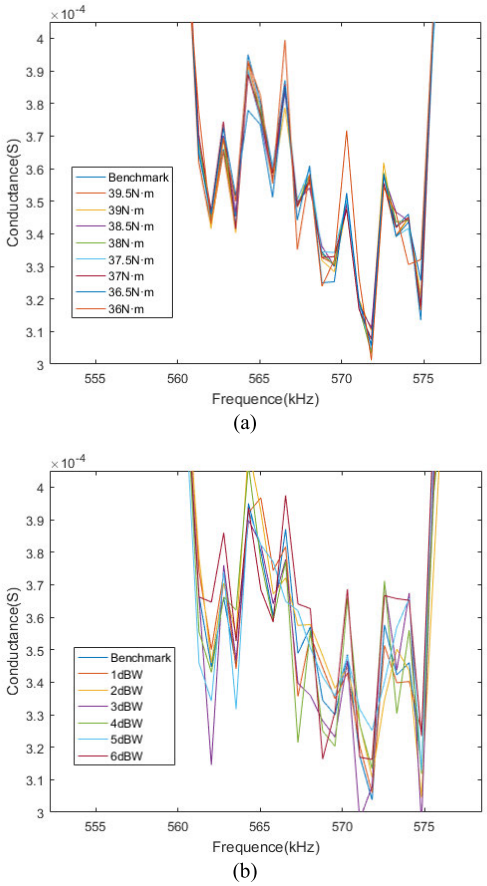

FIGURE 9. The partial enlarged drawing of the conductance spectrum curves under (a) tightening torque of 36 N·m-40 N·m and (b) noise of 1 dBW-6 dBW.

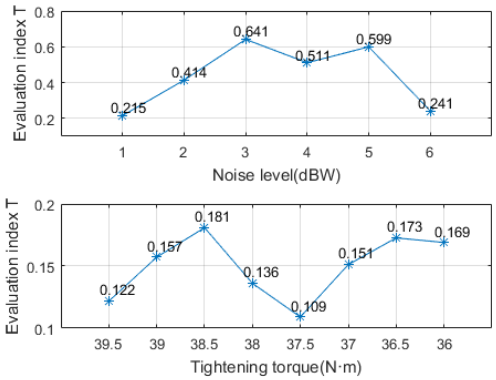

FIGURE 10. Evaluation index T under different working conditions.

In the first picture of Fig. 10, it can be seen that when the noise level changes in the range of 1dBW-6dBW, T fluctuates irregularly in the range of 0.2-0.7. In the second picture, the fluctuation range is 0.1-0.2 when the degree of looseness varies from 36 N·m to 39.5 N·m. The variation range of T in the loose condition is smaller than that in the noise environment, which shows that T can reflect the correlation of the conductance spectrum. By comparing T with the set threshold, the reason for the change of characterization indexes can be judged. When T is greater than 0.2, the reason for

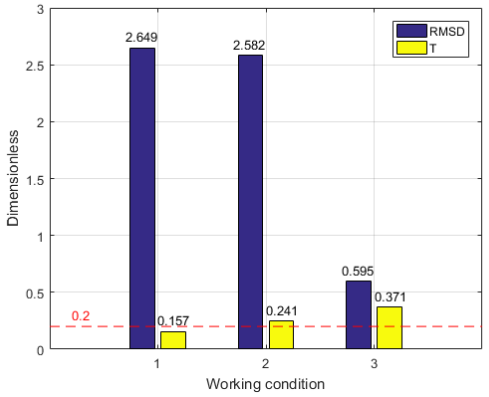

FIGURE 11. T and RMSD under different conditions.

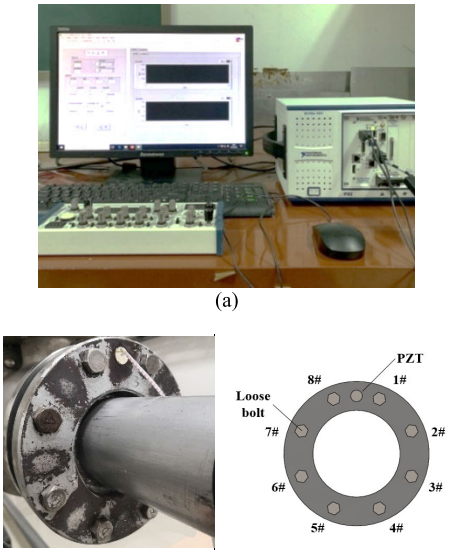

FIGURE 12. The verification experimental devices include (a) a NI data acquisition system and (b) an eight bolted flange with PZT whose layout diagram is shown in (c).

the characterization indexes change is environmental noise. When T is less than 0.2, we can draw the conclusion that the looseness occurred. Fig. 11 shows the RMSD under working condition 1 (36.5 N·m torque, 0 dBW noise) is approximately equal to that under working condition 2 (40 N·m torque, 6 dBW noise). Two different working conditions can be distinguished by comparing T with 0.2 as a threshold value. Working condition 3 is set the same position as the 40 N·m tightening torque in Fig. 9. The RMSD from the measurement is not zero and T is greater than 0.2, indicating that the bolt is not loose and the change of characterization indexes is caused by environmental noise. The conclusion made by T is consistent with the setting condition, which verifies the feasibility of the evaluation index to distinguish noise from actual looseness.

The existing characterization indexes are not able to identify structural looseness and environmental noise. When the indication range of the two cases overlaps, it is more likely to misjudge the looseness only by using

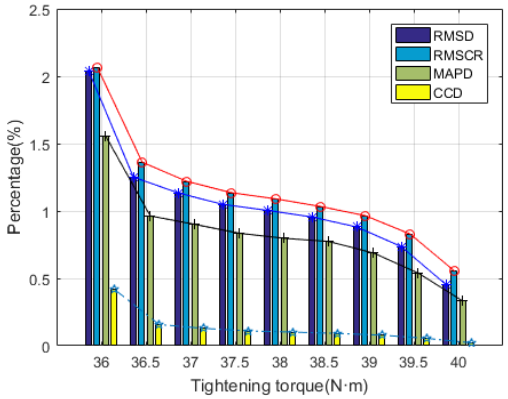

FIGURE 13. Characterization indexes under 36 N·m-40 N·m torque.

TABLE 8. Characterization indexes under different torque.

Torque (N·m)	RMSD	RMSCR	MAPD	CCD	Cov	Cov′
36	2.040	2.061	1.556	0.417	2.50E-06	0.9967
36.5	1.252	1.361	0.963	0.157	2.52E-06	0.9909
37	1.134	1.22	0.900	0.129	2.51E-06	0.9963
37.5	1.049	1.136	0.834	0.110	2.51E-06	0.9948
38	1.004	1.089	0.797	0.101	2.52E-06	0.9974
38.5	0.956	1.033	0.774	0.091	2.52E-06	0.9976
39	0.882	0.965	0.688	0.078	2.52E-06	0.9986
39.5	0.736	0.829	0.540	0.055	2.52E-06	1.0001
40	0.455	0.552	0.331	0.021	2.52E-06	1

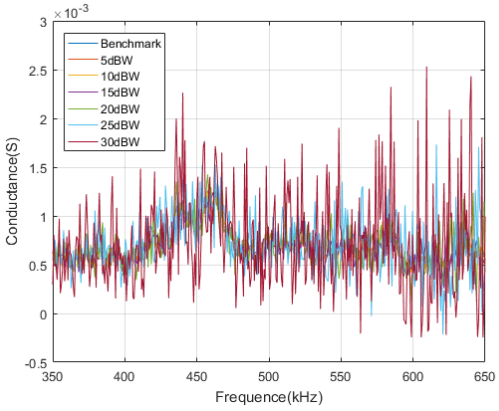

FIGURE 14. The influence of different noise levels 5 dBW-30 dBW on the conductance spectrum.

characterization indexes. We can use T to judge whether the flange bolt occurs slightly loose by determining the threshold value of each flange, establishing the looseness parameter database, and comparing the measured evaluation indexes with the threshold value, which has a strong practical value.

V. VERIFICATION EXPERIMENT

To further study whether the evaluation index is applicable to other flange bolts, the following verification experiment was designed. It is based on an online monitoring system composed of an NI data acquisition system and LabVIEW software control program. The NI data acquisition system

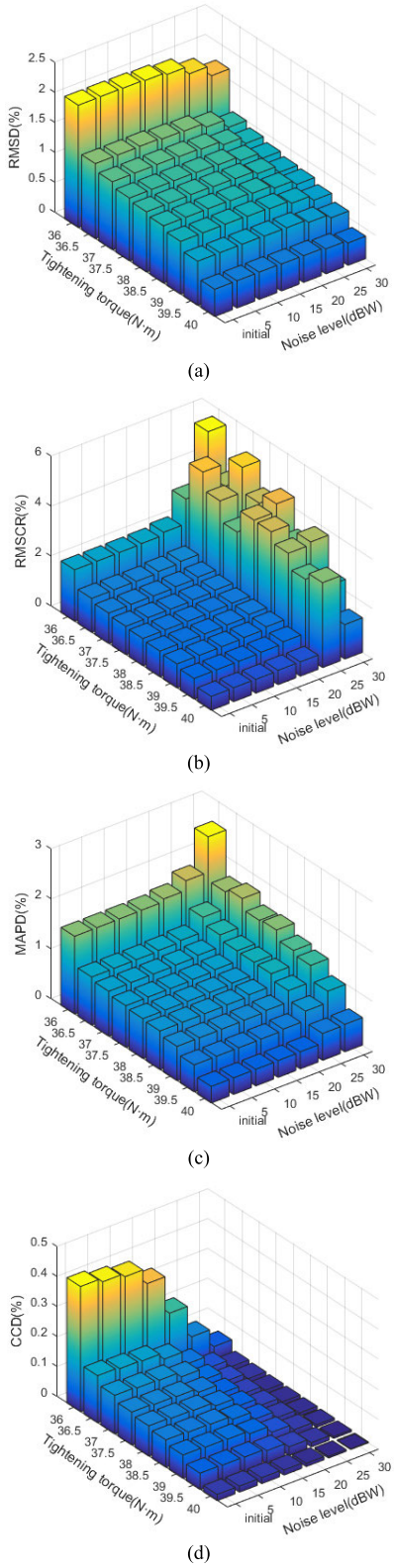

FIGURE 15. Recognition effect of (a) RMSD, (b) RMSCR, (c) MAPD, and (d) CCD on bolt looseness (36 N·m-40 N·m) under 5 dBW-30 dBW noise.

includes PXIe-1071 chassis, PXIe-8840 controller, PXIe-6124 high-speed data acquisition card, and BNC-2120 junction box, as shown in Fig. 12(a). The sampling rate of the

TABLE 9. Characterization indexes under different noise levels.

Noise (dBW)	RMSD	RMSCR	MAPD	CCD	Cov′
1	1.512	1.640	1.237	1.002	0.106
2	1.707	1.882	1.424	0.999	0.134
3	1.834	1.957	1.53	1.007	0.156
4	2.189	2.317	1.733	0.999	0.220
5	2.205	2.420	1.811	1.001	0.226
6	2.582	2.813	2.200	0.998	0.305

PXIe-6124 module is 4 MS/s, which is used to collect admittance signals and generate noise. The excitation signal of the system is a linear chirped signal, which is set at 1 V AC excitation voltage.

The test object in Fig. 12(b) is a flange structure with a size of Φ200 mm and eight M18 mm×1.25 mm×50 mm bolts are uniformly distributed. A PZT of PZT-5A with a size of Φ16 mm×1 mm was pasted at the position shown in Fig. 12(c). Bolts were numbered 1 #-8 # in the clockwise direction and randomly the 7 # bolt was selected as the loose bolt. The material properties are shown in Table 1.

The conductance signals with a frequency range of 350 kHz-650 kHz and a step size of 750 Hz were collected. When the bolt is tightened, the torque is 40 N ·m. Eight groups of loose working conditions were set in the order of 39.5 N·m, 39 N·m, …, 36.5 N·m, 36 N·m, and the experimental data were collected in turn. The average value of characterization indexes was obtained by measuring five times under each working condition. Each index is shown in Table 8. The histogram is made to directly reflect the relationship between the torque and characterization indexes without adding noise, in Fig. 13.

According to Fig. 13, with the increase of bolt looseness degree, the first four characterization indexes also increase, while the Cov' index does not show this feature. All of the above indexes can be used to indicate the looseness except Cov. When the torque is 40 N·m, the normalized values of the first four indexes are 0.223, 0.268, 0.231, and 0.050. RMSCR is the largest and CCD is the smallest. The former is more sensitive to noise than the latter.

In NI, we called the WGN function of MATLAB to generate different levels of white Gaussian noise. Six groups of pseudo-random noise with a level of 5 dBW-30 dBW and an interval of 5 dBW were added to the excitation signal. The effect of noise on the conductance spectrum is shown in Fig. 14 and the effect of characterization indexes are shown in Fig. 15.

Compared with RMSCR and MAPD, when the noise level exceeds 30 dBW, the quantitative loosening and anti-interference ability of RMSD and CCD is better than that of RMSCR and MAPD, which verifies the previous experimental results. Therefore, when the environment noise is strong, it is more reliable to evaluate bolt looseness with the first two indexes. When 1 dBW-6 dBW noise was added to the excitation signal, each index effect is shown in Table 9 and Fig. 16.

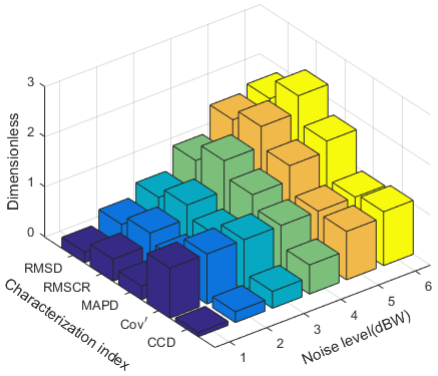

FIGURE 16. Characterization indexes change under the noise of 1 dBW-6 dBW.

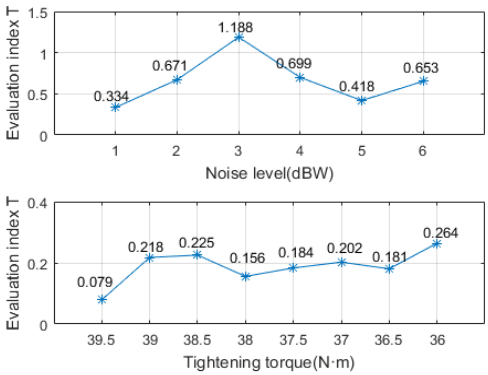

FIGURE 17. Evaluation index T under different working conditions.

By comparing Table 9 with Table 8, it can be concluded that there is a coincidence interval between 1 dBW-6 dBW noise and 36 N·m-39.5 N·m loosening conditions. The calculated value of T is shown in Fig. 17. The recognition range of the evaluation index for noise is 0.3-1.2 and the looseness is 0.07-0.3. We then set the threshold value to 0.3. According to the conductance spectrum of measurement at 40 N·m, T is 0.434 and is greater than the threshold value, which means that the change of characterization indexes is caused by noise and it is consistent with the experimental condition.

Through the experimental study of two different flange bolt specifications, it is found that the state of flange bolt could not be accurately judged when the characterization indexes overlapped under looseness and different noise levels. The correlation characteristics between the conductance spectrum of the benchmark and the conductance spectrum under various working conditions are extracted by the evaluation index T. The results show the efficiency of evaluation index T to distinguish minor looseness from noise.

VI. CONCLUSION

On the basis of the electromechanical impedance method, this paper makes a comparative study on the detection effect of flange bolt looseness with different characterization indexes by monitoring the admittance of PZT pasted on the flange surface, comparing the correlation between the conductance spectrum and benchmarks under different

working conditions. The recognition effect of the proposed evaluation index T is verified by experiments. The specific conclusions are as follows:

Firstly, RMSD, RMSCR, MAPD, and CCD can identify the minor looseness of a bolt in different degrees, and the indicated value has a positive correlation with the looseness degree, whereas Cov cannot reflect the above laws, so it is not feasible to use Cov for the minor looseness identification.

Secondly, the sensitivity of different characterization indexes to environmental noise is different. In the initial state, by comparing the normalized indexes under the benchmark, it can be preliminarily judged that RMSCR has a strong sensitivity to noise and CCD has weak sensitivity to noise. With the increase of noise level, RMSD and CCD show better sensitivity and anti-interference ability to bolt loosening than RMSCR and MAPD. The first two can accurately extract structural features.

Thirdly, a new evaluation index T is constructed to make up for the problems that it is impossible to distinguish minor looseness (36 N·m-39.5 N·m) from noise (1 dBW-6 dBW) with the current characterization indexes because the indication range of the above two conditions overlaps. Index T pays more attention to the correlation difference between the conductance spectrum curves under the benchmark and other conditions. By extracting the correlation feature of the curves with T, we found that there is a different indication range for the minor looseness and noise. The indication range at flange with four bolts is 0.1-0.2 for looseness and 0.2-0.7 for noise. As for the flange with eight bolts, it ranges from 0.07 to 0.3 and 0.3 to 1.2 respectively. By calculating the evaluation index of an unknown condition and comparing it with the set threshold, we can judge whether the bolt looseness has occurred.

The important application significance of the evaluation index T proposed in this study is to improve the ability of bolt loosening identification in the critical state. By setting a threshold to distinguish looseness from noise, the probability of false alarm caused by environmental noise is greatly reduced. The experimental results show that the evaluation index provides a reference for the determination of minor damage to other engineering structures. For future works, the way to extract accurate and effective structural information under a variety of environmental interference coupling fields, determination of the position and degree of multiple loose bolts, as well as the new signal processing technology applied in SHM at low SNR can be studied.

REFERENCES

[1] W. Na and J. Baek, "A review of the piezoelectric electromechanical impedance based structural health monitoring technique for engineering structures," *Sensors*, vol. 18, no. 5, p. 1307, Apr. 2018, doi: 10.3390/s18051307.

[2] A. Cuc, V. Giurgiutiu, S. Joshi, and Z. Tidwell, "Structural health monitoring with piezoelectric wafer active sensors for space applications," *AIAA J.*, vol. 45, no. 12, pp. 2838–2850, 2007, doi: 10.2514/1.26141.

[3] X. Liu and Z. Jiang, "Design of a PZT patch for measuring longitudinal mode impedance in the assessment of truss structure damage," *Smart Mater. Struct.*, vol. 18, no. 12, Dec. 2009, Art. no. 125017, doi: 10.1088/0964-1726/18/12/125017.

[4] S. Fan, W. Li, Q. Kong, Q. Feng, and G. Song, "Monitoring of pin connection loosening using eletromechanical impedance: Numerical simulation with experimental verification," *J. Intell. Mater. Syst. Struct.*, vol. 29, no. 9, pp. 1964–1973, 2018, doi: 10.1177/1045389x18754354.

[5] N. Kaur, L. Li, S. Bhalla, and Y. Xia, "A low-cost version of electro-mechanical impedance technique for damage detection in reinforced concrete structures using multiple piezo configurations," *Adv. Struct. Eng.*, vol. 20, no. 8, pp. 1247–1254, Aug. 2017, doi: 10.1177/1369433216677124.

[6] G. Park, H. H. Cudney, and D. J. Inman, "Feasibility of using impedance-based damage assessment for pipeline structures," *Earthq. Eng. Struct. Dyn.*, vol. 30, no. 10, pp. 1463–1474, 2001, doi: 10.1002/eqe.72.

[7] T. Wang, G. Song, Z. Wang, and Y. Li, "Proof-of-concept study of monitoring bolt connection status using a piezoelectric based active sensing method," *Smart Mater. Struct.*, vol. 22, no. 8, Aug. 2013, Art. no. 087001, doi: 10.1088/0964-1726/22/8/087001.

[8] Y. Zhang, X. Zhang, J. Chen, and J. Yang, "Electro-mechanical impedance based position identification of bolt loosening using Lib-SVM," *Intell. Autom. Soft Comput.*, vol. 24, no. 1, pp. 81–88, 2018, doi: 10.1080/10798587.2016.1267245.

[9] J. Shao, T. Wang, Z. Wang, D. Wei, and Y. Li, "Bolt looseness detection using piezoelectric impedance frequency shift method," *China Mech. Eng.*, vol. 30, no. 12, pp. 1395–1399 and 1408, 2019.

[10] F. Wang, L. Huo, and G. Song, "A piezoelectric active sensing method for quantitative monitoring of bolt loosening using energy dissipation caused by tangential damping based on the fractal contact theory," *Smart Mater. Struct.*, vol. 27, no. 1, Jan. 2018, Art. no. 015023, doi: 10.1088/1361-665x/aa9a65.

[11] L. Huo, F. Wang, H. Li, and G. Song, "A fractal contact theory based model for bolted connection looseness monitoring using piezoceramic transducers," *Smart Mater. Struct.*, vol. 26, no. 10, Oct. 2017, Art. no. 104010, doi: 10.1088/1361-665x/aa6e93.

[12] S. Ritdumrongkul and Y. Fujino, "Identification of the location and level of damage in multiple-bolted-joint structures by PZT actuator-sensors," *J. Struct. Eng.*, vol. 132, no. 2, pp. 304–311, Feb. 2006, doi: 10.1061/(ASCE)0733-9445(2006)132:2(304).

[13] I. Pavelko, V. Pavelko, S. Kuznetsov, and I. Ozolinsh, "Bolt-joint structural health monitoring by the method of electromechanical impedance," *Aircr. Eng. Aerosp. Technol.*, vol. 86, no. 3, pp. 207–214, Apr. 2014, doi: 10.1108/aeat-01-2013-0006.

[14] H. Yin, T. Wang, D. Yang, S. Liu, J. Shao, and Y. Li, "A smart washer for bolt looseness monitoring based on piezoelectric active sensing method," *Appl. Sci.*, vol. 6, no. 11, p. 320, Oct. 2016, doi: 10.3390/app6110320.

[15] M. Rabiei, J. Sheldon, and C. Palmer, "An impedance-based approach for detection and quantification of damage in cracked plates and loose bolts in bridge structures," *Proc. SPIE*, vol. 8348, Apr. 2012, Art. no. 834828, doi: 10.1117/12.915453.

[16] S. K. Samantaray, S. K. Mittal, P. Mahapatra, and S. Kumar, "An impedance-based structural health monitoring approach for looseness identification in bolted joint structure," *J. Civil Struct. Health Monitor.*, vol. 8, no. 5, pp. 809–822, Nov. 2018, 10.1007/s13349-018-0307-2.

[17] T. Tang, M. Hua, X. Jiang, Y. Zhang, and X. Zhang, "Research on improved damage index for evaluating bolt looseness of flange," *J. Beijing Univ. Aeronaut. Astronaut.*, to be published, doi: 10.13700/j.bh.1001-5965.2019.0649.

[18] A. Martowicz, A. Sendecki, M. Salamon, M. Rosiek, and T. Uhl, "Application of electromechanical impedance-based SHM for damage detection in bolted pipeline connection," *Nondestruct. Test. Eval.*, vol. 31, no. 1, pp. 17–44, Jan. 2016, doi: 10.1080/10589759.2015.1058376.

[19] A. Bastani, H. Amindavar, M. Shamshirsaz, and N. Sepehry, "Identification of temperature variation and vibration disturbance in impedance-based structural health monitoring using piezoelectric sensor array method," *Struct. Health Monit., Int. J.*, vol. 11, no. 3, pp. 305–314, May 2012, doi: 10.1177/1475921711427486.

[20] L. M. Campeiro, R. Z. da Silveira, and F. G. Baptista, "Impedance-based damage detection under noise and vibration effects," *Struct. Health Monitor.*, vol. 17, no. 3, pp. 654–667, May 2018, doi: 10.1177/1475921717715240.

[21] B. A. de Castro, F. G. Baptista, and F. Ciampa, "Comparative analysis of signal processing techniques for impedance-based SHM applications in noisy environments," *Mech. Syst. Signal Process.*, vol. 126, pp. 326–340, Jul. 2019, doi: 10.1016/j.ymssp.2019.02.034.

[22] B. A. de Castro, F. G. Baptista, J. A. Ardila Rey, and F. Ciampa, "A chromatic technique for structural damage detection under noise effects based on impedance measurements," *Meas. Sci. Technol.*, vol. 30, no. 7, Jul. 2019, Art. no. 075601, doi: 10.1088/1361-6501/ab0fe2.
[23] B. A. de Castro, F. G. Baptista, and F. Ciampa, "New signal processing approach for structural health monitoring in noisy environments based on impedance measurements," *Measurement*, vol. 137, pp. 155–167, Apr. 2019, doi: 10.1016/j.measurement.2019.01.054.
[24] B. Xu and F. Jiang, "Concrete-steel composite girder bolt loosening monitoring using electromechanical impedance measurements," *Earth Space*, pp. 629–634, 2012, doi: 10.1061/9780784412190.067.
[25] D. Wang and H. Zhu, "Monitoring of the strength gain of concrete using embedded PZT impedance transducer," *Construct. Building Mater.*, vol. 25, no. 9, pp. 3703–3708, Sep. 2011, doi: 10.1016/j.conbuildmat.2011.04.020.
[26] C. Liang, F. P. Sun, and C. A. Rogers, "Coupled electro-mechanical analysis of adaptive material systems-determination of the actuator power consumption and system energy transfer," *J. Intell. Mater. Syst. Struct.*, vol. 8, no. 4, pp. 335–343, Apr. 1997, doi: 10.1177/1045389x9700800406.
[27] S.-W. Zhou, C. Liang, and C. A. Rogers, "An impedance-based system modeling approach for induced strain actuator-driven structures," *J. Vib. Acoust.*, vol. 118, no. 3, pp. 323–331, Jul. 1996, doi: 10.1115/1.2888185.
[28] A. N. Zagrai and V. Giurgiutiu, "Electro-mechanical impedance method for crack detection in thin plates," *J. Intell. Mater. Syst. Struct.*, vol. 12, no. 10, pp. 709–718, Oct. 2001, doi: 10.1177/104538901320560355.
[29] Y. Yang, J. Xu, and C. K. Soh, "Generic impedance-based model for structure-piezoceramic interacting system," *J. Aerosp. Eng.*, vol. 18, no. 2, pp. 93–101, Apr. 2005, doi: 10.1061/(ASCE)0893-1321.
[30] V. Giurgiutiu and C. Rogers, "Recent advancements in the electromechanical (E/M) impedance method for structural health monitoring and NDE," *Proc. SPIE*, vol. 3329, Jul. 1998, Art. no. 316923, doi: 10.1117/12.316923.
[31] H. W. Park, "Evolution of electromechanical admittance of piezoelectric transducers on a timoshenko beam from wave propagation perspective," *J. Intell. Mater. Syst. Struct.*, vol. 28, no. 9, pp. 1221–1245, May 2017, 10.1177/1045389x16667555.
[32] F. P. Sun, Z. Chaudhry, C. Liang, and C. A. Rogers, "Truss structure integrity identification using PZT sensor-actuator," *J. Intell. Mater. Syst. Struct.*, vol. 6, no. 1, pp. 134–139, Jan. 1995, 10.1177/1045389x9500600117.
[33] V. Giurgiutiu, "Structural health monitoring (SHM) of aerospace composites," in *Polymer Composites in the Aerospace Industry*. Salt Lake City, UT, USA: Academic, 2015, pp. 449–507, doi: 10.1016/b978-0-85709-523-7.00016-5.
[34] V. K. Sharma, S. Hanagud, and M. Ruzzene, "Damage index estimation in beams and plates using laser vibrometry," *AIAA J.*, vol. 44, no. 4, pp. 919–923, Apr. 2006, doi: 10.2514/1.19012.
[35] R. Tawie and H. K. Lee, "Monitoring the strength development in concrete by EMI sensing technique," *Construct. Building Mater.*, vol. 24, no. 9, pp. 1746–1753, Sep. 2010, doi: 10.1016/j.conbuildmat.2010.02.014.
[36] F. I. Ferreira, P. R. de Aguiar, R. B. da Silva, M. J. Jackson, R. de Souza Ruzzi, F. G. Baptista, and E. C. Bianchi, "Electromechanical impedance (EMI) measurements to infer features from the grinding process," *Int. J. Adv. Manuf. Technol.*, vol. 106, nos. 5–6, pp. 2035–2048, Jan. 2020, 10.1007/s00170-019-04733-8.
[37] J. Wu, W. Li, and Q. Feng, "Electro-mechanical impedance (EMI) based interlayer slide detection using piezoceramic smart aggregates—A feasibility study," *Sensors*, vol. 18, no. 10, p. 3524, 2018, doi: 10.3390/s18103524.
[38] J. L. Rickli and J. A. Camelio, "Damage detection in assembly fixtures using non-destructive electromechanical impedance sensors and multivariate statistics," *Int. J. Adv. Manuf. Technol.*, vol. 42, nos. 9–10, pp. 1005–1015, Jun. 2009, doi: 10.1007/s00170-008-1657-4.
[39] T.-C. Huynh and J.-T. Kim, "Quantification of temperature effect on impedance monitoring via PZT interface for prestressed tendon anchorage," *Smart Mater. Struct.*, vol. 26, no. 12, Dec. 2017, Art. no. 125004, doi: 10.1088/1361-665x/aa931b.
[40] J. Min, S. Park, and C.-B. Yun, "Impedance-based structural health monitoring using neural networks for autonomous frequency range selection," *Smart Mater. Struct.*, vol. 19, no. 12, Dec. 2010, Art. no. 125011, doi: 10.1088/0964-1726/19/12/125011.
[41] G. Park, K. Kabeya, H. Cudney, and D. Inman, "Removing effects of temperature changes from piezoelectric impedance-based qualitative health monitoring," *Proc. SPIE*, vol. 3330, Jul. 1998, Art. no. 316963, doi: 10.1117/12.316963.
[42] S. Na and H. K. Lee, "A multi-sensing electromechanical impedance method for non-destructive evaluation of metallic structures," *Smart Mater. Struct.*, vol. 22, no. 9, Sep. 2013, Art. no. 095011, doi: 10.1088/0964-1726/22/9/095011.
[43] Y. Yang, Y. Hu, and Y. Lu, "Sensitivity of PZT impedance sensors for damage detection of concrete structures," *Sensors*, vol. 8, no. 1, pp. 327–346, Jan. 2008, doi: 10.3390/s8010327.
[44] Y. Hu and Y. Yang, "Wave propagation modeling of the PZT sensing region for structural health monitoring," *Smart Mater. Struct.*, vol. 16, no. 3, pp. 706–716, Jun. 2007, doi: 10.1088/0964-1726/16/3/018.
[45] W. Yan and W. Q. Chen, "Structural health monitoring using high-frequency electromechanical impedance signatures," *Adv. Civil Eng.*, vol. 2010, pp. 1–11, 2010, doi: 10.1155/2010/429148.
[46] H. Zhu, H. Luo, D. Ai, and C. Wang, "Mechanical impedance-based technique for steel structural corrosion damage detection," *Measurement*, vol. 88, pp. 353–359, Jun. 2016, doi: 10.1016/j.measurement.2016.01.041.
[47] B. A. de Castro, F. G. Baptista, and F. Ciampa, "New imaging algorithm for material damage localisation based on impedance measurements under noise influence," *Measurement*, vol. 163, Oct. 2020, Art. no. 107953, doi: 10.1016/j.measurement.2020.107953.
[48] B. A. de Castro, F. G. Baptista, and F. Ciampa, "A comparison of signal processing techniques for impedance-based damage characterization in carbon fibers under noisy inspections," *Mater. Today: Proc.*, to be published, doi: 10.1016/j.matpr.2020.03.470.

XIE JIANG received the bachelor's degree from the Xi'an Research Institute of Hi-Tech, in 2019, where he is currently pursuing the master's degree in mechanical engineering. His research interests include structural health monitoring, smart materials and structures, and analytical/numerical modeling.

XIN ZHANG received the master's and Ph.D. degrees in vehicle failure physics and reliability from the Xi'an Research Institute of Hi-Tech, in 2015 and 2020, respectively. He is currently a Lecturer with the Xi'an Research Institute of Hi-Tech. His research interests include intelligent detection, online monitoring, and pattern recognition of mechanical and electrical systems.

YUXIANG ZHANG received the Ph.D. degree in system engineering from Xi'an Jiaotong University, in 1998. From 1999 to 2003, he held a postdoctoral research position with Xi'an Jiaotong University and the Chinese Academy of Sciences. He is currently a Professor with the Xi'an Research Institute of Hi-Tech. His current research interests include the areas of intelligent detection, fault diagnosis, and information technology.